THERMAL ANALYSIS OF Mg DOPED ZnO NANO PARTICLES AS FILLER IN EPOXY FOR THERMAL INTERFACE MATERIAL IN LED PACKAGING

S.SHANMUGAN*, D.MUTHARASU
Nano Optoelectronics Research Laboratory, School of Physics, UniversitiSains Malaysia (USM), 11800, Minden, Pulau Pinang, Malaysia

Mg doped ZnO nano particles (MZO) were synthesized with various Mg concentrations by co-precipitation method and used as filler in epoxy for LED performance. The prepared samples were also annealed to see the effect of temperature on thermal resistance and also thermal conductivity of synthesized samples. Thermal transient analysis was used to study the performance of Mg doped ZnO as filler in epoxy with high power LED. Low total thermal resistance ($R_{th\text{-}tot}$) and raise in junction temperature (T_J) were noticed with 2M% MZO annealed at 500°C. The observed results were evaluated by measuring the thermal conductivity of MZO for various Mg concentrations and achieved high values with 2M% MZO samples annealed at 500°C. Mg concentration was influenced the thermal conductivity of ZnO nano particles and also improved the same with moderate concentration. Annealed temperature was also supported to reduce the thermal resistance and to improve the thermal conductivity of Mg doped ZnO nano particles. Overall, Mg doped ZnO nano particle will be used as good filler for thermal interface material application in electronic packaging industry.

(Received November 26, 2015; Accepted January 11, 2016)

Keywords: LED; Magnesium; ZnO; Thermal Transient Analysis; Thermal conductivity

1. Introduction

Maintenance of ideal working temperature by removing the heat dissipated is essential for proper functioning of electronic devices like LED, microprocessors, etc. Due to increasing thermal loads driven by technological advancements, thermal management is becoming a great challenge for high power electronic devices. To improve the efficiency of heat transfer systems, two methods are suggested (i) active mode (increasing coolant velocity and also their thermal conductivity) and (ii) passive modes (use of fins, channels with expansions and constrictions, higher heat transfer area). An LED rated at 50000 hours with a junction temperature of 25°C will survive only half as long with a junction temperature of 125°C.To enhance the heat flow from the hot junction of the LED to atmosphere, conductive particles filled interface material will be used between MCPCB and heat sink to avoid the interfacial thermal resistance effectively.

ZnO is the richest family of nanostructures among all semiconducting materials, both in structures and in properties due to its unique properties [1,2]. Nitride and oxide based materials have been suggested for thermal interface materials (TIM) and thermal paste type TIM has been mostly used for all electronic packaging applications for ease of use. Xu et al., also reported that out of all the commercial thermal interface materials studied, the ZnO filled silicone of Dow Corning gives the highest thermal contact conductance [3]. Kasimiri et al., reported that 50 wt% ZnO samples showed good thermal conductivity behavior similar to the 15 wt% CNT samples [4]. ZnO is also referred as good filler with Al particles in pentaerythritol oleate media for thermal interface material application [5]. The same author group has already reported the performance of LED using metal oxide as filler mixed with commercial thermal paste and achieved noticeable results [6].

*Corresponding author: shagan77in@yahoo.co.in

The use of dopants not only enhances the conductivity of ZnO material by extrinsic defects but also improves the thermal stability. The thermal treatment and doping process also can lead to the modification of surface morphology which will improve the material quality [7-9]. Various reports of doped ZnO indicate that the doping effect increased the optical and electrical properties of the ZnO [10–11]. Furthermore, the sol concentration also affects the crystalline, optical and electrical properties of ZnO. Literature [12] studied the incorporation of ZnO into epoxy resin for TIM application. The effect of mixing ZnO with Boron Nitride on the thermal conductivity enhancement for phenolic formaldehyde (PF) resin was reported in literature [13] as well. Various chemical synthesis methods have been suggested to synthesize nano / micro crystals such as solvothermal, hydrothermal, self-assembly and Sol-gel, precipitation method etc [14-18]. Among these methods, precipitation method is a simple and cost effective method and used in this study. Mg was selected as dopant to ZnO nano particles and Mg doped ZnO nano particles was synthesized using precipitation method with various Mg concentration. The thermal transient analysis was performed for the given LED employed Mg doped ZnO nano particles as filler in epoxy for thermal interface material application. Thermal conductivity of Mg doped ZnO nano particles was also tested and reported here.

2. Experimental Methodology

2.1. Synthesis of Mg doped ZnO nano particles

Mg doped ZnO nano particles were synthesized by co-precipitation method. Zinc Nitrate Hexahydrate $Zn(NO_3)_2{\cdot}6H_2O$ from Sigma Aldrich, Sodium Hydroxide NaOH from Sigma Aldrich and Magnesium Chloride Hexahydrate $MgCl_2{\cdot}6H_2O$ from QRëC™ were AR grade and used for the synthesis of Mg-doped Zinc Oxide without further purification. For synthesis of pure ZnO, 29.749g of $Zn(NO_3)_2{\cdot}6H_2O$ and 8.00g of NaOH were dissolved separately in 200ml of double distilled water to prepare 0.5M and 1.0 M solutions respectively.

In all the literature, NaOH is added into zinc solution. Instead, the zinc solution is added into the NaOH solution in this study. This is to ensure the dissolution of zinc hydroxide precipitate into zinc complex ion which can serves as self-assembly units as well as providing an alkaline environment for reaction [12]. Consequently, NaOH solution was stirred by mechanical stirrer at 500 rpm and $Zn(NO_3)_2{\cdot}6H_2O$ solution was added dropwise to it and hence form white precipitates. The titration took about 1.5 hours to complete and the resulting solution was allowed to age for 2 hours. The precipitate was then filtered out, washed for 4 times with double distilled water and ethanol successively to remove unwanted solutions. Later, the precursor was dried in oven at 120°C for 4 hours, crushed into powder using ceramic mortar and filtered. The pure ZnO nanopowder was obtained. For Mg doping, $MgCl_2{\cdot}6H_2O$ solution is added along with $Zn(NO_3)_2{\cdot}6H_2O$ and prepared solution.

Table 1. Mass of Magnesium salt required to produce desired doping concentration.

Sample Name	Atomic Percentage (%mol) of Mg dopant	Mass of $MgCl_2{\cdot}6H_2O$ added (g)
0MZO	pure ZnO	-
2MZO	2	0.4149
4MZO	4	0.8471
6MZO	6	1.2977
8MZO	8	1.7679
10MZO	10	2.2590

In order to change the atomic concentration of Mg into the ZnO, the weight of $MgCl_2{\cdot}6H_2O$ was varied and mixed with $Zn(NO_3)_2{\cdot}6H_2O$ to achieve the doping concentration as mentioned in table – 1. Later, the as-synthesized and Mg doped samples were annealed at two different temperatures (500°C and 700°C) in a furnace for about 2 hours at air atmosphere with the heating rate of 10°C/min. For sample naming, the sample name in which the front number

represents the Mg doping percentage and the number behind represent the annealing temperatures of the sample. For example 2MZO-5 represents 0.2 M% Mg doped ZnO annealed at 500°C. Hereafter, the sample name is pronounced based on this nomenclature.

2.2. Thermal Transient Analysis

Before the real measurement, the LED was thermally calibrated using dry thermostat and T3Ster as the power supply. The product of K and the difference in temperature-sensing voltage (referred to as ΔVF) produces the device junction temperature rise:

$$\Delta T_J = \Delta V_F K \tag{1}$$

During the calibration process, the LED was driven with lower operating current (1mA) to prevent self-heating effect at the junction. The ambient temperature of the LED was fixed to 25˚C and the voltage drop across the junction was recorded once the LED reaches thermal equilibrium with the temperature of the thermostat. Later, the ambient temperature of the LED was varied from 35˚C to 85 with 10°C step size and the voltage drop across the junction was noted at each ambient temperature. From the calibration process, the K-factor of the LED was determined from the graph of junction voltage (voltage drop) against ambient temperature as 1.677mV/K.

The thermal transient analysis was carried out for the given LED at 700 mA in a still-air chamber at room temperature. The schematic diagram of testing configuration for high power LED is shown in Fig.1. A LED was forward biased for 600s and the transient cooling curve of heat flow from the LED package was captured for another 600s. The obtained cooling profile of the LED with epoxy and Mg doped ZnO nano particles filled epoxy was processed for structure functions using Trister Master Software and reported.

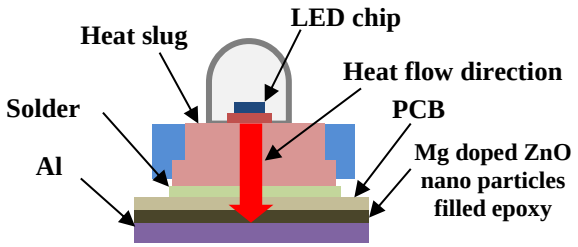

Fig. 1. Schematic diagram of interface material testing configuration

The device junction temperature in the test condition can be determined by

$$T_J = T_{J0} + \Delta T_J \tag{2}$$

where T_{J0} = initial device junction temperature (ºC), ΔT_J = change in junction temperature due to heater power application (ºC). Static mode was applied using still air box for all measurement, which applies heating power to the Device Under Test (DUT) on a continuous basis while the T_J was monitored through measurement of temperature-sensitive parameter.

2.3. Bulk Thermal Conductivity Test

As-synthesized and annealed nano powder samples were made into two pellets for further characterizations. Ethyl cellulose was chosen as the binder because of its low price besides it was readily available in the laboratory. The bulk thermal conductivity of the pellets were characterized using Hot Disk® TPS 2500S Thermal Constants Analyzer. The annealing process was performed after preparing the pellet where the binder was evaporated during the process.

2.3. Preparation of TIM

0.05g of Bisphenol A Diglycidyl Ether (DGEBA) which is a main component of epoxy resin, was weighed and the sample powder was mixed thoroughly with it in the ratio of 5:1. The resulting mixture was spread uniformly on the bottom part of the metal core printed circuit board (MCPCB) of LED which is then attached to an aluminum heat sink. A contact pressure is applied by G-clamp in order to reduce the air gaps as well as to avoid unexpected dislocations during the measurement.

3. Results and Discussion

3.1. Thermal Transient Analysis

The cumulative structure function analysis curve of the given LED was recorded for different boundary conditions as shown in fig. 2. In order to see the detailed changes in curve at ambient side of the device, the data are magnified and given as inset for discussion in the same fig.2.

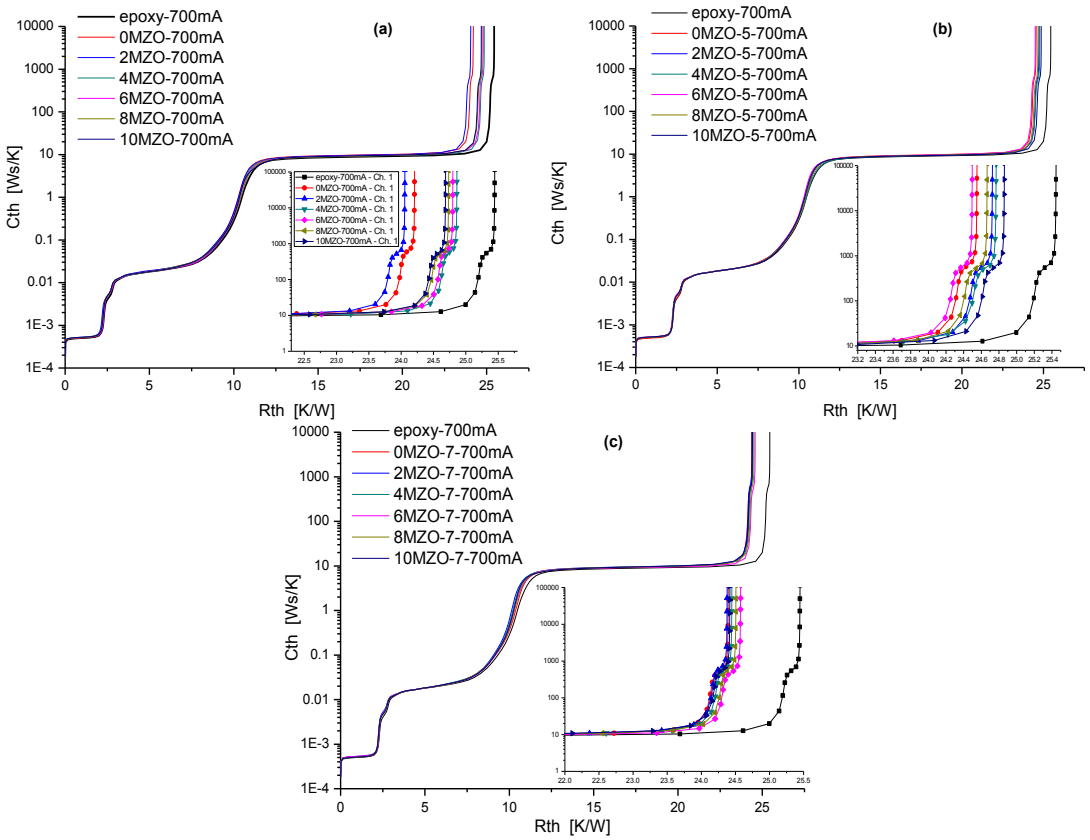

Fig. 2. Cumulative structure function of LED under Mg doped ZnO nano particles filled epoxy as thermal interface material with various Mg concentrations

From the inset fig.2, it is clearly understood that the Mg concentration plays a significant role on changing the $R_{th\text{-}tot}$ of the given LED and observed low $R_{th\text{-}tot}$ value with 2MZO boundary conditions. Moreover, the inset fig.2 also describes the advantage of Mg doped ZnO over the commercial epoxy as thermal interface application. The fig.2 also explains the influence of Mg doped ZnO after annealing process on $R_{th\text{-}tot}$ of the LED at 700 mA. To elaborate this observation, the $R_{th\text{-}tot}$ values are extracted from the cumulative structure function with the aid of T3Ster Master Software. The derived values are plotted against the various boundary conditions (sample name) as shown in Fig.3.

From the fig.3, it is understood that the $R_{th\text{-}tot}$ of the LED changes with respect to the Mg concentration and also the processing temperatures. Overall, the 10 mole % of Mg doped ZnO nano particles (10MZO) annealed at 500 °C shows high $R_{th\text{-}tot}$ values than as grown and annealed at 700 °C samples.

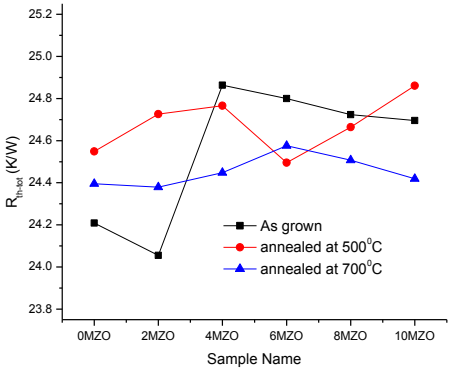

Fig. 3. Variation in $R_{th\text{-}tot}$ of LED for different boundary conditions

This may be due to the effect of structural defects from annealing process. Very low value in $R_{th\text{-}tot}$ is noticed with 2 MZO sample than all other boundary conditions. The Mg concentration greater than 4 mole % shows lower $R_{th\text{-}tot}$ values for annealed samples than as grown samples. Consequently, it is expected that the T_J values of the LED will decrease with reduced $R_{th\text{-}tot}$. To elaborate this observation, the T_J values are measured from the transient cooling curve using the T3Ster Master Software and plotted in Fig.4. Since the change in junction temperature is based on the thermal resistance of the interface materials and hence the trend or pattern of the change in T_J is expected to be the same as observed for $R_{th\text{-}tot}$. Fig.4 exhibits the same pattern as observed for $R_{th\text{-}tot}$. Very low and high values in T_J are observed with 2MZO and 10 MZO samples or boundary conditions respectively. Even though we studied the performance of LED with various boundary conditions, there is not clear information about the thermal resistance of interface materials. Here we used undoped and Mg doped ZnO nano particles filled epoxy as thermal interface materials and the thermal resistance of undoped and Mg doped ZnO particles filled epoxy should be addressed.

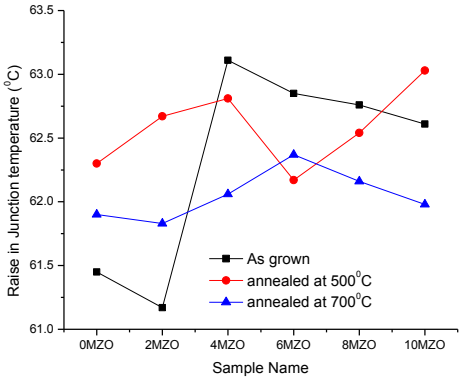

Fig. 4. Variation in raise in junction temperature (T_J) of LED for different boundary conditions

Consequently, the interface thermal resistance was also evaluated from the cumulative structure function and the observed results are plotted in Fig.5. The performance $R_{th\text{-}tot}$ is based on the several factor in which interface thermal resistance plays an important role. The interface thermal resistance will reflect the behavior of $R_{th\text{-}tot}$ and also the T_J variation in the LED will have the same pattern as observed for $R_{th\text{-}tot.}$ The difference in interface thermal resistance ($\Delta R_{th\text{-}b\text{-}hs}$) is very low compared to the $\Delta R_{th\text{-}tot}$.

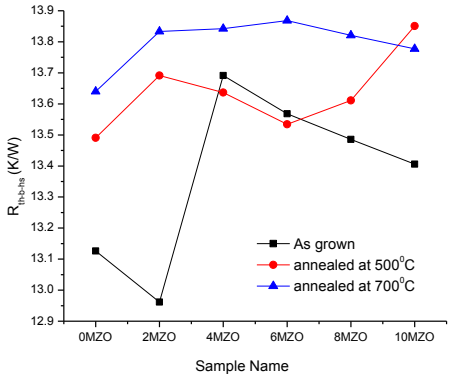

Fig. 5. Variation in thermal resistance of interface material (Mg doped ZnO filled epoxy) for different boundary conditions

3.1. Thermal Conductivity Analysis

Since the interface thermal resistance is very low, it is necessary to disclose the thermal conduction behavior of the undoped and Mg doped ZnO nano particles to understand the importance of the work. To support this evaluation, the thermal conductivity of prepared samples were measured and plotted in fig.6. It clearly explains that the thermal conductivity is changing with respect to the concentration of Mg in ZnO. Moreover, the fig. 6 shows that the thermal conductivity initially decreases for low Mg concentration and increases with high Mg concentration. The improvement of thermal conductivity is noticed with 2MZO samples annealed at 500°C and also observed as high value when compared to all samples. It is understood that the annealing temperature helps to increase the thermal conductivity of the doped ZnO nano particles especially at 500°C. The thermal conductivity values are high for the samples annealed at 500°C than the samples of as grown and annealed at 700°C. This measurement supports the observation of low $R_{th\text{-}tot}$ and low T_J for 2MZO samples and exhibits the suitability of 2MZO sample as thermal interface material for LED application. From these observation, it is concluded that the thermal conductivity and also the performance of Mg doped ZnO nano particles as thermal interface material could be improved by further optimization in synthesis as well as analysis of the same.

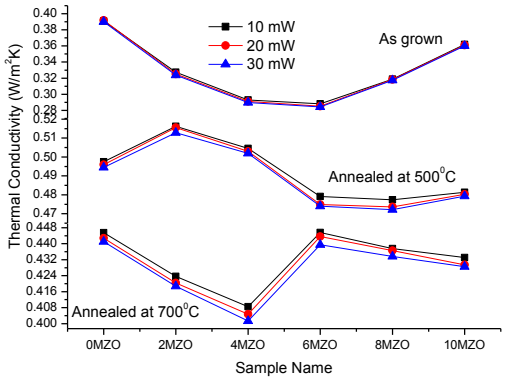

Figure 6. Thermal conductivity of Mg doped ZnO nano particles at various Mg concentration and process conditions

4. Conclusions

Mg doped ZnO nano particles were synthesized by co-precipitation method and used as filler in epoxy for thermal interface materials. Thermal transient analysis was performed for the given LED with the Mg doped ZnO particles filled epoxy as thermal interface materials and observed low $R_{th\text{-}tot}$ for 2MZO sample annealed at 500°C. Consequently, low T_J value was noticed

with same 2MZO sample annealed at 500°C. High value in thermal conductivity was also measured with 500°C annealed Mg doped ZnO nano particles especially for 2 Mol % Mg doped ZnO samples. Overall it is concluded the Mg can be used as dopant for ZnO to improve the thermal conductivity of ZnO and also Mg doped ZnO nano particles could be suggested as good filler for epoxy as thermal interface applications.

Acknowledgments

I express my gratitude to FYP students who have collected the data of thermal transient curves and also thermal conductivity of Mg doped ZnO nano particles.

References

[1] S. Nabizadeh, T. Fanaei sheikholeslami, A. Behzadmehr, Bull. Elect. Engg. and Infor., **2**, 233 (2013)
[2] S. Hotchandani, P.V. Kamat, J. Electrochem. Soc., **139**, 1630 (1992).
[3] S. Sakohapa, L.D. Tickazen, M.A. Anderson, J. Phys. Chem. **96**, 11086 (1992)
[4] Y. Xu, X. Luo and D.D.L. Chung, Tran. of ASME-J. of electro. Pack., **122**, 128 (2000)
[5] M. Kasimir, K. Gharagozloo-Hubmann, S. Trotsenko, G. J. F. Czempiel, V. Datsyuk, S. Reich, Thermal interface materials based on carbon nanotubes and their thermal characterization, 6-8, Barcelona, Spain, October 2010
[6] C.T. Cheng and N.-T. Cheng, http://www.google.com/patents/US20070131897, Jun 14. 2007
[7] S. Shanmugan and D. Mutharasu, International Journal of Power Electronics and Drive Systems, **3**, 409 (2013)
[8] J.H. Lee and B.O. Park, Thin Solid Films**, 426**, 94 (2003).
[9] Y. Yamamoto, K. Saito, K. Takakashi, M. Konagai, Sol. Energy Mater. Sol. Cells, **65**, 125 (2001)
[10] Y. Natsume and H. Sakata, Mater. Chem. Phys. **78**, 170 (2002)
[11] G. Srinivasan. R.T. Rajendra Kumar, J. Kumar, Opt. Mater. **30**, 314 (2007).
[12] E.J.L. Arredondo, A. Maldonado, R. Asomoza, D.R. Acosta, M.A.M. Lira, M. de la, L. Olvera, Thin Solid Films, **490**, 132 (2005).
[13] Y. Fu, Z. He, D. Mo, and S. Lu, Applied Thermal Engineering**, 66**, 493 (2014).
[14] F. Yuan, H. Zhang, X. Li, X. Li, and Z. Yu, Compo. Part A: Appl. Sci. Manufac. **53**, 137 (2013).
[15] B.B. Lakshmi, C.J. Patrissi and C. R. Martin, Chem. Mater. **9**, 2544 (1977).
[16] L. Vayssieres, K. Keis, A. Hagfeldt, S.E. Lindquist, Chem. Mater., **13**, 4395 (2001).
[17] C. Pacholski, A. Kornowski, H. Weller, Angew. Chem. Int. Edn. Engl., **41**, 1188 (2002).
[18] L. Vayssieres, Adv. Mater., **15**, 464 (2003).
[19] B. Liu, H.C. Zeng, J. Am. Chem. Soc., **125**, 4430 (2003).